Molecular-dynamics study of liquid NaPb, KPb, RbPb, and CsPb alloys

H. T. J. Reijers and W. van der Lugt
Solid State Physics Laboratory, Materials Science Centre, University of Groningen, Melkweg 1, 9718 EP Groningen, The Netherlands

Marie-Louise Saboungi
Argonne National Laboratory, Argonne, Illinois 60439-4837

(Received 11 December 1989; revised manuscript received 16 April 1990)

A molecular-dynamics study on equiatomic NaPb, KPb, RbPb, and CsPb liquid alloys has been carried out to supplement earlier neutron-diffraction measurements. The alkali-metal atoms are assumed to be monovalent, positively charged ions while the Pb atoms are arranged in regular tetrahedra, $(Pb_4)^{4-}$, so-called Zintl ions. A simplified version of the Tosi-Fumi potential has been used to represent the interatomic forces, except for the Pb-Pb interactions within a $(Pb_4)^{4-}$ ion, which are approximated by a harmonic potential. The structure factors calculated from this molecular-ionic model prove to be in excellent agreement with the measured ones.

I. INTRODUCTION

Recently, neutron-diffraction measurements have been performed on NaPb, KPb, RbPb, and CsPb liquid-equiatomic alloys.[1] The structure factors are characterized by a first sharp diffraction peak (FSDP) at about 1 $Å^{-1}$, except for NaPb, where the FSDP occurs at 1.3 $Å^{-1}$. The FSDP has been interpreted as an indication for the presence of polyatomic structural units.[1] This explanation agrees nicely with the model previously presented by Geertsma *et al.*[2] and by Van der Lugt and Geertsma[3] to account for the shift in stoichiometry observed in among others the resistivity[4] and the Darken excess stability function.[5] According to this model the tetrahedral polyanions $(Pb_4)^{4-}$ or Zintl ions observed in the crystal structure of NaPb (Ref. 6) as well as in those of KPb, RbPb, and CsPb (Ref. 7) persist upon melting. A picture of the unit cell of the crystal structure of NaSn, which is isomorphous, with those of NaPb, KPb, RbPb, and CsPb can be found in Ref. 8. Geertsma and Dijkstra[9] have pointed out that due to the relatively large size of the alkali-metal atoms, the formation of Pb_4 tetrahedra is energetically more favorable than a structure in which the Pb atoms are evenly distributed over the liquid. However, this argument does not apply to Li-Pb because of the small size of Li atoms. This explains why the maximum in the resistivity occurs at 80 at. % alkali metal in Li-Pb, while it has shifted towards the equiatomic composition for K-Pb, Rb-Pb, and Cs-Pb. The system Na-Pb proves to be intermediate between Li-Pb and K-Pb: the resistivity shows a maximum at 80 at. % Na as well as a small hump at 50 at. % Na.

To obtain a more-detailed understanding of the structure and deduce additional information, we have attempted to simulate these liquids by molecular dynamics (MD). We have opted to incorporate Pb_4 tetrahedra in our calculations since the primary purpose of our MD study has been to find out if a model based on Pb_4 tetrahedra is able to fit the experimentally determined structure factors. Analysis of the electronic transport properties,[2,3] band-structure calculations,[8] and comparison with the crystal structure[6,7] has led us to the conclusion that $(Pb_4)^{4-}$ ions are the most likely units to occur. Therefore, we have not attempted to use any other unit in our MD study. A code developed by Rahman for MD simulations of the tetrachloroaluminates[10] has been used as a starting point for our MD program.

II. MOLECULAR-DYNAMICS CALCULATIONS

While there is extensive literature about MD simulations in the field of molten salts available (see, e.g., the review paper by Sangster and Dixon[11]), hardly any MD work has been carried out for liquid metals and alloys. Pioneering work has been done by Rahman,[12] who has studied liquid Rb. Using an interparticle potential that has an oscillatory decay to zero, he found that density fluctuations occur for wavelengths as short as the nearest-neighbor distance. The alkali metals Na and Cs have been investigated by Lee *et al*,[13] the alloys $Na_{0.60}Cs_{0.40}$ and $Na_{0.85}Cs_{0.15}$ by Huijben *et al.*[14] In these studies the effective interatomic potential has been calculated within the framework of the pseudopotential approximation. Jacucci *et al.*[15] have carried out a MD simulation for Li_4Pb, using a pair potential proposed by Copestake *et al.*,[16] of which the parameters have been derived from the experimentally determined ordering potential. Recently, Hafner[17] has tried to simulate the structure of liquid KPb by MD, using first-principles pseudopotential theory and a modified linear screening approach. He has shown that large clusters of Pb atoms are formed due to a strongly attractive ionic pseudopotential between Pb atoms. However, quantitative agreement with the experimental data is poor. A major breakthrough has been achieved by Car and Parrinello,[18] who have combined MD technique with Hohenberg-Kohn-Sham density-functional theory. This implies an extension of MD beyond the usual pair-potential approxima-

tion and allows the simulation of both covalently bonded and metallic systems.

In the present work we have assumed that the A atoms (A =Na, K, Rb, or Cs) donate an electron to the Pb atoms and become singly charged ions. The Pb^- ions have been grouped in clusters of four ions. The ions within a cluster can vibrate around their equilibrium positions, which together constitute a regular tetrahedron. Thus our system consists of a mixture of A^+ and $(Pb_4)^{4-}$ ions. The pair potential ϕ_{ij} between particles i and j, if they are not Pb^- ions belonging to the same tetrahedron, is a Born-Mayer-Huggins-type (BMH) potential:[19]

$$\phi_{ij}(r)=b_{ij}\exp[a(d_{ij}-r)]+\frac{z_i z_j e^2}{r} , \tag{1}$$

where

$$b_{ij}=b_0\left[1+\frac{z_i}{n_i}+\frac{z_j}{n_j}\right] . \tag{2}$$

Here, r is the interparticle distance, d_{ij} is the short-range interaction diameter of ions i and j, a and b_0 are parameters characterizing the short-range repulsion, z_i and z_j are the charges of ions i and j, e is the elementary charge, and n_i and n_j are the numbers of electrons in the outer shells of ions i and j (8 for A^+ and 5 for Pb^-). This potential differs from the original one used by Tosi and Fumi in their work on the solid alkali-metal halides[20] in that the two terms representing the van der Waals interactions have been dropped. The Pb-Pb interactions within $(Pb_4)^{4-}$ are approximated by a harmonic potential:

$$\phi_{ij}(r)=\tfrac{1}{2}c(r-d_0)^2 , \tag{3}$$

where c is the force constant and d_0 the distance between the equilibrium sites.

The MD simulations were carried out for systems consisting of a total number of 256 particles, contained in a cubic box. The side L of the box was chosen to yield the densities mentioned in Table I, which were taken from Ref. 1. The time step used was $\Delta t=10^{-15}$ s and was sufficiently small to ensure conservation of energy. The usual periodic boundary conditions were imposed on the system. For the calculation of the force on a given particle, only those particles lying within a cubic box of side L and with that particle as its center were considered. An initial configuration was created by placing the particles at a random position within the box. In the case of Pb_4 tetrahedra, their centers of mass were given a random position after which the Pb particles were put at the corners of a tetrahedron of side d_0. Starting from this configuration, a series of consecutive configurations was subsequently generated using the "leap-frog" algorithm of Verlet[21] to find the new positions and velocities after each time step. A temperature T was defined by putting the total kinetic energy of a particular configuration equal to $\frac{3}{2}Nk_BT$, where k_B is Boltzmann's constant and N is the total number of particles. If the calculated temperature T_{calc} exceeded a preset range around the required temperature T_{req}, the displacements of the particles were rescaled by a factor $(T_{\text{req}}/T_{\text{calc}})^{1/2}$. The initial temperatures were usually several thousand degrees kelvin. Therefore, several short runs were performed to allow the system to reach equilibrium before the actual simulation was started. Typically a total number of 1000 steps was needed for this purpose. After that a "production" run of 5000 steps was carried out during which the temperature fluctuated around the set temperature and the displacements of the particles were not rescaled. To estimate effects due to the finite size of the box, we have performed a MD simulation for KPb with 2048 particles in a cubic box twice as large. A starting configuration was created by a combination of eight identical boxes containing an equilibrium configuration of 256 particles in such a way that they formed a new cubic box of side 2 L. The pair and triplet correlation functions as well as the structure factors obtained from this larger system were essentially the same as the ones found for the smaller system. This has led us to the conclusion that our sample of 256 particles is sufficiently representative as far as the structural properties are concerned.

To avoid inaccuracies due to the slow convergence of the long-range Coulomb forces, the well-known Ewald summation technique[22] has been employed. This method was originally developed for the calculation of the Madelung contribution to the lattice energy of ionic crystals. Regarding the box used in MD as the unit cell of a simple cubic lattice, we find by applying the Ewald summation method that the total Coulomb potential of particle i in the field of the other particles can be transformed into two rapidly converging series:

$$\phi_i^{(1)}=\sum_j\sum_{\mathbf{n}} z_i z_j\frac{\operatorname{erfc}[\alpha r_{ij}(\mathbf{n})]}{r_{ij}(\mathbf{n})}-\frac{z_i^2\alpha}{\sqrt{\pi}} , \tag{4a}$$

where the complementary error function is given by

TABLE I. Densities, temperatures, and parameters of the potential used in the MD simulations.

	ρ_0 (Å^{-3})	T (K)	a (Å^{-1})	d_{AA} (Å)	$d_{A\text{Pb}}$ (Å)	d_{PbPb} (Å)	d_0 (Å)
NaPb	0.0308	680	3.0	3.77	3.53	3.70	3.30
KPb	0.0217	870	3.0	2.66	3.75	4.84	3.25
RbPb	0.0192	880	2.5	2.96	3.90	4.84	3.20
CsPb	0.0168	930	2.0	3.38	4.11	4.84	3.15
	$b_{AA}=0.423\times10^{-12}$ erg				$z_A=+1$		
	$b_{A\text{Pb}}=0.313\times10^{-12}$ erg				$z_{\text{Pb}}=-1$		
	$b_{\text{PbPb}}=0.203\times10^{-12}$ erg				$c=0.8$ mdyn/Å		

$$\mathrm{erfc}(x)=1-\mathrm{erf}(x)=1-\int_0^x \exp(-u^2)du \ , \tag{4b}$$

and

$$\phi_j^{(2)}=\frac{1}{\pi L}\sum_j \sum_{\mathbf{n}(\neq 0)} z_i z_j \frac{\exp(-\pi^2|\mathbf{n}|/\alpha^2 L^2)}{|\mathbf{n}|^2} \times\cos[2\pi\mathbf{n}\cdot\mathbf{r}_{ij}(\mathbf{n})] \ . \tag{4c}$$

Here, $\mathbf{n}$ is the vector (in units of L) specifying the position of the box in which particle j lies with respect to the box containing particle i, thus $\mathbf{r}_{ij}(\mathbf{n})=(\mathbf{r}_j+\mathbf{n}L)-\mathbf{r}_i$. In the calculations $\phi_j^{(1)}$ was truncated at $r=L/2$ and $\phi_j^{(2)}$ at $|\mathbf{n}|=6$, with $\alpha L=5$.

At the end of the MD simulation the following quantities were obtained (in the following two paragraphs the subscripts α, β, and γ refer to chemical species).

(1) The pair-correlation functions $g_{\alpha\beta}(r)$ for $r<L/2$ (α-β= A-A, A-Pb, Pb-Pb, CM-A, CM-Pb, and CM-CM, where CM refers to the center of mass of the Pb_4 tetrahedra), defined by

$$\langle n_{\alpha\beta}(r)\rangle \Delta r=4\pi r^2 \Delta r \rho_\beta g_{\alpha\beta}(r) \ . \tag{5}$$

Here, $n_{\alpha\beta}(r)\Delta r$ is the number of β particles at distance r from an α particle lying in a shell between $r-\Delta r/2$ and $r+\Delta r/2$, and ρ_β is the number density of β particles. The brackets $\langle\ \rangle$ denote an average over all configurations as well as an average over α particles. We have used $\Delta r=0.05$ Å.

(2) The coordination numbers $Z_{\alpha\beta}$ defined by

$$Z_{\alpha\beta}=\frac{\sum_z z\langle n_{\alpha\beta}^{(z)}\rangle}{n_\alpha} \ . \tag{6}$$

Here, $n_{\alpha\beta}^{(z)}$ is the number of α particles having precisely z particles of type β up to the distance defined by the minimum following the first peak in $g_{\alpha\beta}(r)$, and n_α is the total number of α particles. The subscript "α-β" and the angular brackets have the same meaning as in Eq. (5).

(3) The triplet correlation functions $N_{\alpha\beta\gamma}(\theta)$ for A-A-A, Pb-Pb-Pb, A-Pb-A, Pb-A-Pb, A-A-Pb, A-Pb-Pb, A-CM-A, Pb-CM-Pb, and A-CM-Pb triplets. It gives the distribution of triplets over the cosines of the angles θ defined as the angle that the line connecting a β particle with an α particle makes with the line connecting that same β particle with a γ particle.

(4) The self-diffusion constants D_α ($\alpha=A$,Pb,CM) calculated from the mean-square-displacement using the Einstein formula

$$D_\alpha=\lim_{t\to\infty}\frac{\langle|\mathbf{r}_\alpha(t)-\mathbf{r}_\alpha(0)|^2\rangle}{6t} \ , \tag{7}$$

where $\langle\ \rangle$ denotes an average over all α particles.

The partial structure factors $S_{\alpha\beta}(q)$ were obtained by Fourier transformation of the pair-correlation functions $g_{\alpha\beta}(r)$ according to

$$S_{\alpha\beta}(q)=\delta_{\alpha\beta}+4\pi(\rho_\alpha\rho_\beta)^{1/2}\int_0^\infty r^2[g_{\alpha\beta}(r)-1]\frac{\sin(qr)}{qr}dr \ . \tag{8}$$

The pair-correlation functions were truncated at $r=L/2$, which corresponds to a distance of at least 10 Å. By comparison of the partial structure factors of KPb obtained from the MD simulation with 256 particles on the one hand, with those obtained from the "big" MD simulation using 2048 particles on the other hand, it follows that there are no differences between the two sets of partial structure factors except for the small q range (below 0.5 $Å^{-1}$), which is not of interest to us. Therefore, effects due to truncation in the Fourier transformation can be left out of consideration. The partial structure factors and pair correlation functions were subsequently combined to yield the total structure factor and the radial distribution function, respectively, for comparison with the neutron-diffraction data:

$$S(q)=\frac{\sum_{\alpha,\beta} b_\alpha b_\beta(\rho_\alpha\rho_\beta)^{1/2}S_{\alpha\beta}(q)}{\sum_\alpha \rho_\alpha b_\alpha^2} \tag{9}$$

and

$$N(r)=\frac{\rho_0\sum_{\alpha,\beta} b_\alpha b_\beta\rho_\alpha\rho_\beta 4\pi r^2 g_{\alpha\beta}(r)}{\left[\sum_\alpha \rho_\alpha b_\alpha\right]^2} \ , \tag{10}$$

where $\rho_0=\sum_\alpha\rho_\alpha$ denotes the total number density and where b_α and b_β are the scattering lengths of α and β taken from a compilation by Sears.[23]

TABLE II. Short-range interaction diameters.

	d_{AA}[a] (Å)	d_{APb}[a] (Å)	d_{PbPb}[a] (Å)	d_{AA}[b] (Å)	d_{APb}[b] (Å)	d_{PbPb}[b] (Å)
NaPb	3.77	3.53	3.70	1.90	3.37	4.84
KPb	4.23	4.01	4.39	2.66	3.75	4.84
RbPb	4.33	4.15	4.67	2.96	3.90	4.84
CsPb	4.58	4.42	5.08	3.38	4.11	4.84

[a]Based on crystal distances corrected for thermal expansion.
[b]Based on Pauling radii.

III. RESULTS AND DISCUSSION

A. Choice of parameters

The parameters of the potential have been chosen such that the MD simulations yield a reasonable description of the structure factors obtained from the neutron-diffraction experiments and are given in Table I. For b_0 the same value as adopted by Tosi and Fumi has been used: $b_0 = 0.338 \times 10^{-12}$ erg. The value of a has been adjusted to make the heights of the main peaks in the structure factors of both the MD simulations and the experimental data agree with each other. The values of a become smaller in the order NaPb, KPb, RbPb, and CsPb, implying that the short-range repulsion becomes softer. This is to be expected since the larger the alkali atom, the more deformable it is. Two ways of obtaining the interaction diameters were considered (see Table II). In the first attempt the average A-A, A-Pb, and Pb-Pb nearest-neighbor distances (the intratetrahedron Pb-Pb distance was excluded from the averaging) taken from the crystal structure and corrected for thermal expansion were used. In the second attempt the diameters were set equal to the sum of the Pauling ionic radii.[24] The most important difference between the two sets of diameters is that the values of d_{AA} derived from the crystal are much larger than the corresponding diameters based on the Pauling radii. For KPb, RbPb, and CsPb the latter choice turned out to be the best, while for Na-Pb the first set of diameters worked better. The finally adopted values are given in Table I. The value of c has been found by comparing the damping of the high-q oscillations of the calculated structure factors with the experimental results. Satisfactory agreement is obtained if c is chosen to be

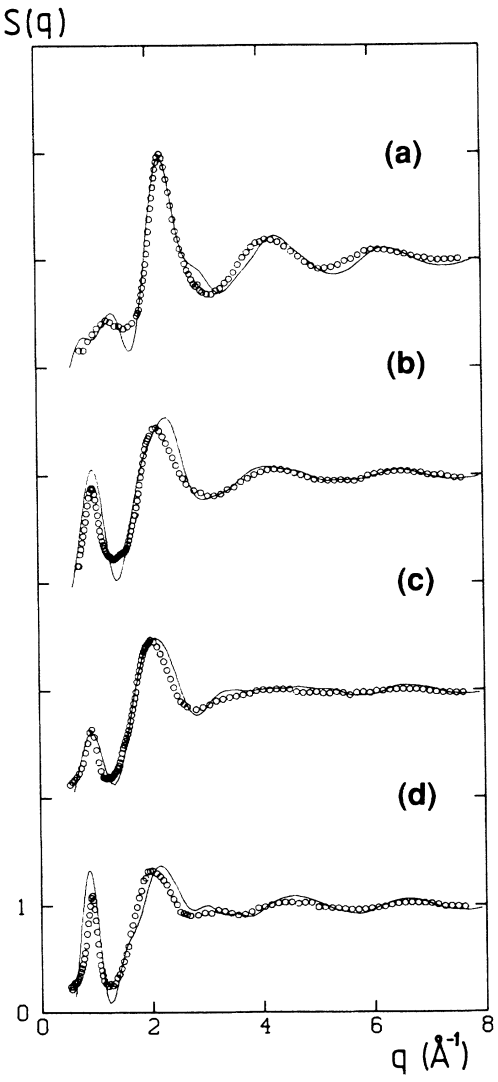

FIG. 1. Structure factors $S(q)$ found by neutron-diffraction experiment and MD simulation. The curves are the MD results, the open circles are the neutron data: (a) NaPb at 680 K, (b) KPb at 870 K, (c) RbPb at 880 K, and (d) CsPb at 930 K.

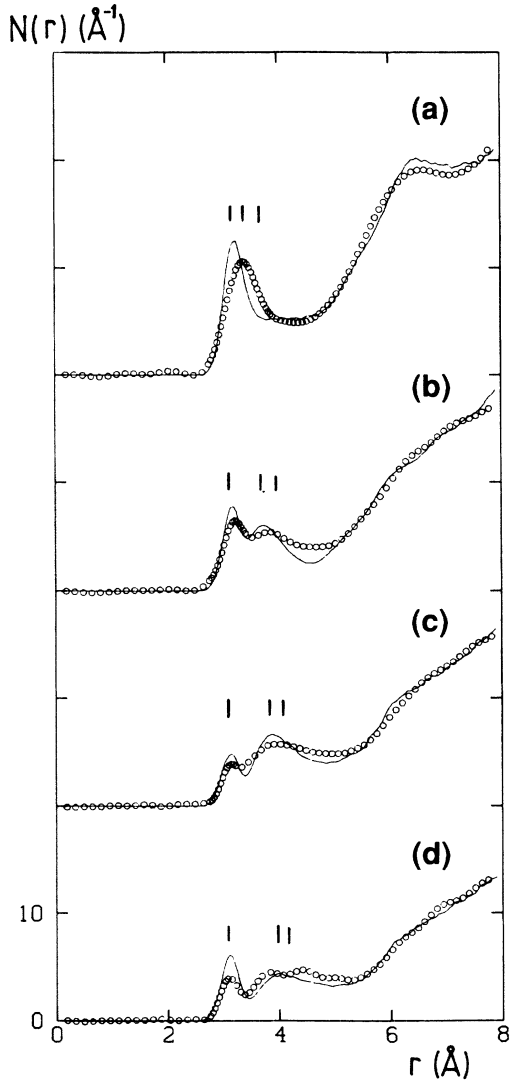

FIG. 2. Radial distribution functions $N(r)$ found by MD simulation as well as neutron-diffraction measurements. The curves are the MD results, the open circles refer to the neutron experiments: (a) NaPb at 680 K, (b) KPb at 870 K, (c) RbPb at 880 K, and (d) CsPb at 930 K. The vertical bars denote (in order of increasing r) the average Pb-Pb, A-Pb, and A-A nearest-neighbor distances in the crystal.

TABLE III. Prepeak positions of NaPb for different x values, where x is the fraction of Pb^- ions forming Pb_4 tetrahedra.

x	q_p (Å^{-1})
0.0	1.50
0.25	1.44
0.5	1.38
0.75	1.32
1.0	1.11

0.8 mdyn/Å. This is of the same order of magnitude as the values of the optically determined force constants of Si—Si and Ge—Ge bonds in $(Si_4)^{4-}$ and $(Ge_4)^{4-}$ tetrahedra, respectively.[25] Similarly, the bond lengths d_0 have been chosen to match the periods of the high-q oscillations of the measured structure factors. Note that apart from CsPb they are slightly larger than the positions of the first peaks in experimentally determined $T(r)=4\pi\rho_0 r g(r)$,[1] where ρ_0 is the number density and $g(r)$ the total pair-correlation function.

B. Structure factors and radial distribution functions

Figures 1 and 2 show the structure factors $S(q)$ and the radial distribution functions $N(r)$ calculated from the MD simulations together with the experimental results. We have assumed that all Pb^- ions are clustered in tetrahedra except for NaPb, which will be discussed in the next section.

KPb, RbPb, and CsPb. Confining ourselves to KPb, RbPb, and CsPb for the moment, we see that the positions of the FSDP are correctly predicted, although its height is slightly overestimated for KPb and CsPb. The high-q side of the main peak of the computed $S(q)$ has been shifted to the right with respect to the peak of the experimental $S(q)$. The agreement between the high-q oscillations of both the measured and calculated structure factors is satisfactory. Inspection of the partial structure factors (see Fig. 4) shows that these oscillations are due mainly to the Pb-Pb correlations. In the same way it turns out that the small satellite peak of Cs-Pb at about 3 Å^{-1} is also a Pb-Pb peak.

The total radial distribution functions found in the MD simulations show the typical two-peak structure in the first coordination shell (i.e., the region between 3 and 5 Å) which is characteristic for clustering systems.[1] The peak at smaller r corresponds with an intracluster distance, the peak at larger r with an intercluster distance. The vertical bars in Fig. 2 indicate the nearest-neighbor distances in the crystal. In order of increasing r they correspond with the Pb-Pb, A-Pb, and A-A distance. The positions of the first peak at about 3.1 Å coincide nicely with the Pb-Pb distances of the solid. The next peak is related to the A-Pb and A-A distances, which are not resolved, but show up as a single broad peak both in the calculations and the measurements, except for the experimentally obtained $N(r)$ of Cs-Pb.

NaPb. The NaPb system proved to be the most difficult system to simulate. As pointed out in the Introduction, Na-Pb is intermediate between Li-Pb, in which the Pb^- ions are more evenly distributed, and K-Pb, which shows clustering. Therefore, it is likely that only a fraction x of the Pb^- ions forms tetrahedra in NaPb. We have performed simulations of NaPb for $x=1$, 0.75, 0.5, 0.25, and 0. In this sequence the position of the first peak in $S(q)$ increases gradually from 1.11 to 1.50 Å^{-1} (see Table III). This can be understood as follows. The intertetrahedron Pb-Pb distance in a fully clustered system is larger than the Pb-Pb distance in an even distribution. Thus, the average Pb-Pb distance decreases when the fraction of tetrahedra becomes smaller. The best agreement with the experimental $S(q)$ was obtained for $x=0.75$. The main peak of the measured $S(q)$ is very well represented by the simulations, while the high-q oscillations are slightly out of phase. The position of the first peak in the $N(r)$ derived from the experimental $S(q)$ is underestimated by the MD results.

TABLE IV. Positions of the first maximum (r_1) and minimum (r_2) of the pair-correlation functions and the corresponding coordination numbers Z.

	A-A			A-Pb			Pb-Pb		
	r_1 (Å)	r_2 (Å)	Z	r_1 (Å)	r_2 (Å)	Z	r_1 (Å)	r_2 (Å)	Z
NaPb	3.90	5.3	8.9	3.24	4.5	6.8	3.12	3.6	2.3
KPb	4.3	6.0	8.7	3.69	5.1	6.9	3.15	3.8	3.0
RbPb	4.38	6.1	8.5	3.93	5.2	6.7	3.09	4.0	3.0
CsPb	4.80	6.4	8.3	3.93	5.4	6.1	3.09	4.0	3.0
solid			7.5			7			3
	CM-Pb			CM-A			CM-CM		
	r_1 (Å)	r_2 (Å)	Z	r_1 (Å)	r_2 (Å)	Z	r_1 (Å)	r_2 (Å)	Z
NaPb	1.88	2.3	4.0	3.42	4.5	7.2	6.60	8.7	7.8
KPb	1.93	2.3	4.0	4.38	5.0	7.7	7.61	10.0	12.3
RbPb	1.89	2.3	4.0	4.50	5.2	8.0	7.92	10.5	12.5
CsPb	1.89	2.3	4.0	4.50	5.5	7.7	8.26	11.0	12.3
solid			4			8			12

C. Partial pair-correlation functions and structure factors

We will now consider the pair-correlation functions in more detail. Fig. 3 shows the A-A, A-Pb, and Pb-Pb pair-correlation functions. The vertical bars denote the nearest-neighbor distances calculated from the known crystal structure using the parameters from Ref. 1. The positions of the first peak, r_{max}, as well as the coordination numbers Z found by integration up to the minimum r_{min} following the first peak are exhibited in Table IV. For comparison we have also included the corresponding coordination numbers of the solid, in this case defined as the number of β atoms within a sphere of radius r_{min} around an α atom where r_{min} has the same value as above. It turns out that these coordination numbers are the same for NaPb, KPb, RbPb, and CsPb.

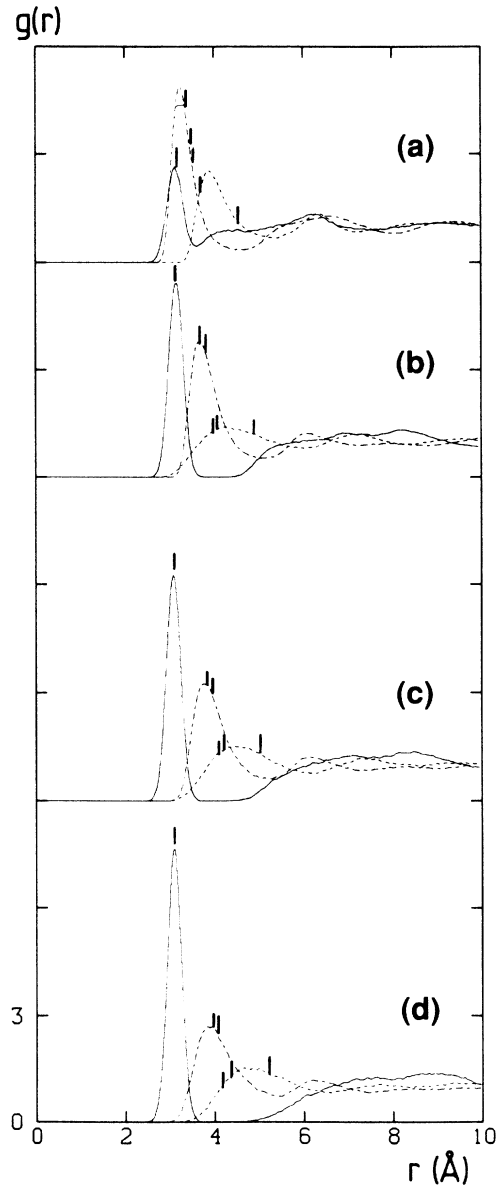

FIG. 3. Pair-correlation functions of Pb-Pb (solid), A-A (dashes), and A-Pb (long-short dashes) correlations: (a) NaPb at 680 K, (b) KPb at 870 K, (c) RbPb at 880 K, and (d) CsPb at 930 K. The vertical bars denote the corresponding nearest-neighbor distances in the crystal.

KPb, RbPb and CPb. Comparing the partials of Fig. 3 we note certain systematic variations. We see that $g_{AA}(r)$ is gradually displaced to the right in the sequence KPb, RbPb, and CsPb. This is a consequence of the increasing size of the alkali ions. In the same order the height of the first peak of $g_{A\mathrm{Pb}}(r)$ decreases because the short-range repulsion becomes softer, which is reflected by a decrease of the a values. Its position is determined by the minimum of the interaction potential between A^+ and Pb^- ions. The first peak of $g_{\mathrm{PbPb}}(r)$ becomes higher, narrower, and better separated from the next peak in the above-mentioned sequence. It seems that the larger the alkali ions, the less freely the Pb^- ions within a tetrahedron can move. Besides, the values of the peak position are slightly smaller than the values used for d_0 (see Tables I and IV). The Pb_4 tetrahedra are compressed under the influence of the surrounding particles. Note that the positions of the first peak of the A-A, A-Pb, and Pb-Pb partials agree nicely with the distances in the solid.

NaPb. Comparing the pair-correlation functions of NaPb with those of KPb, RbPb, and CsPb, we note the following differences. The height of the first peak of $g_{\mathrm{PbPb}}(r)$ has become smaller. Besides, there is no region between the first and second peak where $g_{\mathrm{PbPb}}(r)$ becomes zero like in those of KPb, RbPb, and CsPb. The height of the first peak of $g_{\mathrm{NaNa}}(r)$ has increased and the position of the first peak of $g_{\mathrm{NaPb}}(r)$ has shifted towards smaller r. These differences are consequences of the facts that only a fraction of the Pb^- ions is clustered and that the number density of NaPb is larger than those of KPb, RbPb, and CsPb.

The partial structure factors $S_{AA}(q)$, $S_{A\mathrm{Pb}}(q)$, and $S_{\mathrm{PbPb}}(q)$ are plotted in Fig. 4. The part below 0.8 $Å^{-1}$ is not shown because of spurious oscillations due to truncation errors. Clearly, the FSDP is due to the Pb-Pb partial, which exhibits a huge peak at about 1 $Å^{-1}$, except for NaPb, where it occurs at 1.4 $Å^{-1}$. The height of this peak is increasing in the order KPb, RbPb, and CsPb. In order to establish a relation between the peaks of the pair-correlation functions and their Fourier transforms, we make use of the extrema of the integrand of Eq. (8),[26] $[r^2\sin(qr)/qr]$, which has maxima at $qr=2.03$, 7.98, 14.21, etc., and minima at $qr=4.91$, 11.09, etc. This is a simplified analysis since the influence of higher Fourier harmonics is not considered. We confined ourselves to the partials of KPb. Analogous relations can be established for RbPb and CsPb. The Pb-Pb peak at 3.1 Å is expected to give rise to a maximum at $q=7.98/3.1\approx 2.6$ $Å^{-1}$. At this position an asymmetry can be observed at the right side of a peak in $S_{\mathrm{PbPb}}(q)$ at 2.4 $Å^{-1}$, which becomes more pronounced when going from KPb to CsPb as a consequence of the increase in height of the first peak in $g_{\mathrm{PbPb}}(r)$. The broad maximum in $g_{\mathrm{PbPb}}(r)$ centered around 8 Å yields the high and narrow peak at $q=7.98/8\approx 1$ $Å^{-1}$, which is responsible for the FSDP. The peak in $g_{\mathrm{KPb}}(r)$ at 3.8 Å should contribute to a minimum of $S_{\mathrm{KPb}}(q)$ near $q=4.91/3.8\approx 1.3$ $Å^{-1}$, while

the maximum in $g_{KK}(r)$ at 4.1 Å gives rise to the peak at 1.9 $Å^{-1}$.

We have tried to estimate the contribution of the peak in $g_{PbPb}(r)$ at 3.1 Å to $S_{PbPb}(q)$ by comparing the Fourier transforms of $g_{PbPb}(r)$ with and without first peak. It turns out that the peak at 1 $Å^{-1}$ is essentially the same in both cases. The high-q oscillations of $S_{PbPb}(q)$ are strongly damped when the first peak of $g_{PbPb}(r)$ is left out. Similarly we have left out the part of $S_{PbPb}(q)$ below 1.5 $Å^{-1}$ and compared its Fourier transform with the one obtained from the complete $S_{PbPb}(q)$. The peak of $g_{PbPb}(r)$ at 3.1 Å is hardly affected. The difference of the two transforms obtained from the complete $S_{PbPb}(q)$ and without including the part below 1.5 $Å^{-1}$ yields a long-wavelength Fourier component of which the amplitude has a maximum at about 7.3 Å. From this follows that the first peak of $S_{PbPb}(q)$ is related to distances between Pb atoms that are not lying within the same tetrahedron but belong to neighboring tetrahedra.

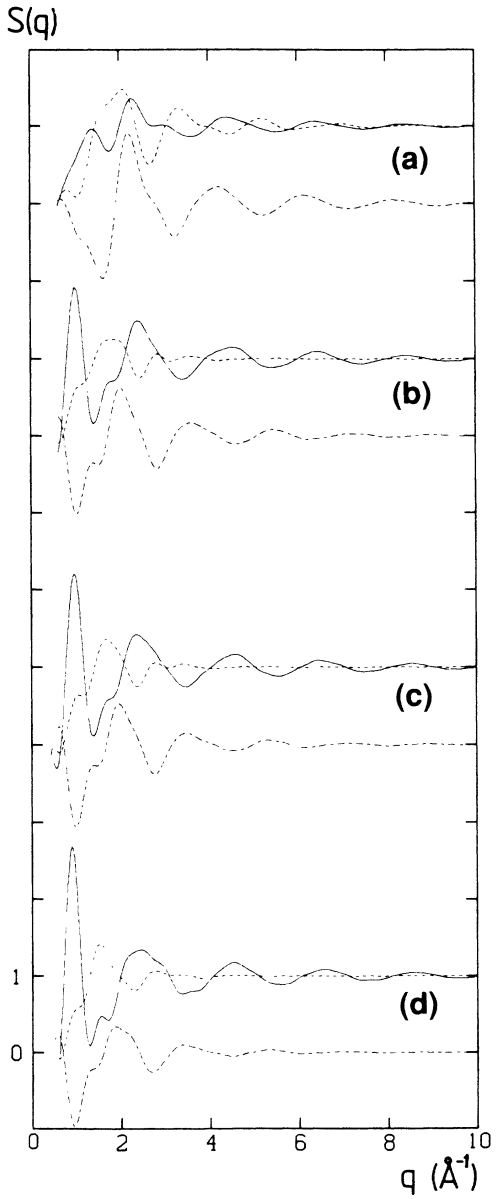

FIG. 4. Partial structure factors of Pb-Pb (solid), A-A (dashes), and A-Pb (long-short dashes) correlations found by Fourier transformation of the corresponding pair-correlation functions of Fig. 3.

D. Pair-correlation functions involving the center of mass and coordination numbers

Since useful information on a molecular system is expected to be obtained from correlations of the centers of mass of the molecules, we have also calculated pair-correlation functions for CM-Pb, CM-A, and CM-CM, which are shown in Fig. 5. For practical reasons we have left out the first peak of $g_{CMPb}(r)$ since its height attains values larger than 30. Just as before, the vertical bars refer to the corresponding distances in the solid.

KPb, RbPb, and CsPb. Again, we can observe certain

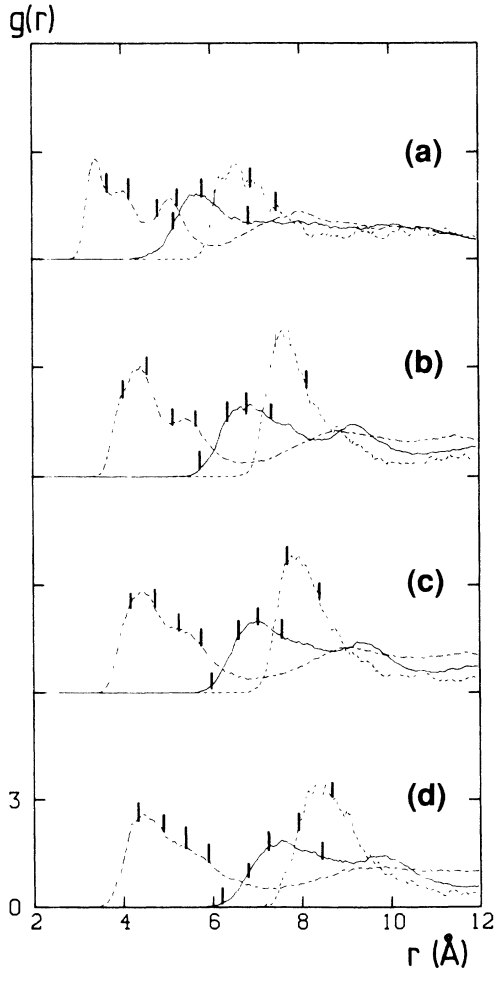

FIG. 5. Pair-correlation functions of CM-Pb (solid), CM-CM (dashes), and CM-A (long-short dashes) correlations: (a) NaPb at 680 K, (b) KPb at 870 K, (c) RbPb at 880 K, and (d) CsPb at 930 K. The vertical bars denote the corresponding nearest-neighbor distances in the crystal.

tendencies in the sets of partials for KPb, RbPb, and CsPb. The first peak of $g_{CMA}(r)$ shows a splitting for KPb, which has become weaker for RbPb and has disappeared in CsPb, although it is still strongly asymmetric. This implies that there are two preferred CM-A distances between which the distinction becomes systematically smaller in the order KPb, RbPb, and CsPb. Indeed there are two sets in the solid, each consisting of two CM-A distances. The average distance of each set coincides more or less with the positions of both subpeaks as shown in Fig. 5 by vertical bars. From inspection of the crystal structure follows that there are alkali atoms sitting opposite the centers of the faces of a Pb_4 tetrahedron as well as alkali atoms opposite the corners. The former atoms are closer to the center of mass than the latter ones. Thus we can distinguish two shells of alkali ions in the liquid surrounding a tetrahedron. The inner shell contains those A^+ ions close to the faces of the tetrahedron, the outer shell those near the corners.

In the foregoing discussion we have seen that there is good agreement in general between peak positions and nearest-neighbor distances in the solid. The same can be said about the correspondence between coordination numbers of KPb, RbPb, and CsPb in both solid and liquid. The Pb-Pb and CM-Pb coordination numbers have of course the values 3 and 4, respectively. The A-A and A-Pb coordination numbers of the liquid are slightly smaller than those of the solid and decrease systematically from KPb to CsPb. The CM-A and CM-CM coordination numbers are, respectively, nearly equal to and smaller than the corresponding values in the solid. The values of these coordination numbers observed in the solid, 8 and 12, respectively, can be interpreted as follows. The centers of mass of the Pb_4 tetrahedra in the crystal constitute a body-centered tetragonal lattice in which each lattice point is surrounded by twelve other points. From the sixteen A atoms that surround a particular tetrahedron,[7] four are situated opposite the centers of the faces of the tetrahedron, four are located opposite four edges of the tetrahedron, four are nearly opposite the corners of the Pb_4 tetrahedron, and 4 other A atoms are arranged in pairs above and below the tetrahedron. The former eight are closer to the center of mass than the latter eight. This explains why we arrive at a coordination number of 8 if we integrate up to that distance where the splitting or asymmetry in $g_{CMA}(r)$ occurs and at about twice that value if we integrate over the whole peak.

NaPb. The partial pair-correlation functions of NaPb involving the center of mass show differences compared with those of KPb, RbPb, and CsPb. The peak of $g_{CMPb}(r)$ at about 5.7 Å is not followed by a second peak. Three peaks lying close to each other can be observed in $g_{CMNa}(r)$. The first and second peak are centered around 3.8 Å and together yield a coordination number of 7.2, which is almost the same as the coordination numbers calculated from the left half of the double peak observed in the $g_{CMA}(r)$'s of KPb, RbPb, and CsPb (see Table IV). If the third peak is also included in the calculation of the coordination number, we get a value that is just twice as large. The separation between the various distances of the Na^+ ions surrounding a particular tetrahedron on the one hand and its center of mass on the other hand is apparently more pronounced for NaPb than for KPb, RbPb, and CsPb. This is probably related to the small size of the Na^+ ions. Both the position and the height of the first peak of $g_{CMCM}(r)$ have decreased.

E. Triplet correlation functions

Figure 6 shows the nine triplet correlation functions for KPb. We have not included those of NaPb, RbPb, and CsPb since the analysis of NaPb becomes too complex due to the simultaneous presence of Pb^- and $(Pb_4)^{4-}$ ions, while the results of RbPb and CsPb are quite similar to those of KPb. The vertical bars are the cosines of the

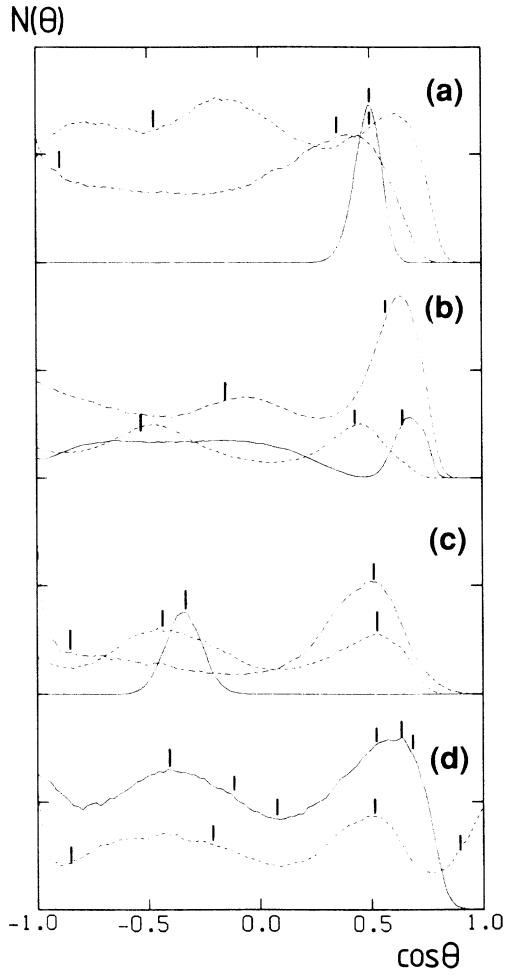

FIG. 6. Triplet correlation functions of KPb. (a) Pb-Pb-Pb (solid), K-K-K (dashes), and K-Pb-K (long-short dashes) triplets. (b) Pb-K-Pb (solid), Pb-Pb-K (dashes), and Pb-K-K (long-short dashes) triplets. (c) Pb-CM-Pb (solid), K-CM-K (dashes), and Pb-CM-K (long-short dashes) triplets. (d) K-CM-K (solid) and Pb-CM-K (dashes) triplets using the second minimum in $g_{CMK}(r)$ as cutoff distance. The vertical bars denote the corresponding values of $\cos\theta$ calculated using the values of the positions of the first peak of the pair-correlation functions shown in Figs. 3 and 5 and, in some cases, also those of the second peak. Arbitrary units have been used along the vertical axis.

angles calculated using the values of the position corresponding to the first peak of the pair-correlation functions and, in some cases, also those of the second peak. The Pb-Pb-Pb correlation function shows a well-defined peak at $\cos\theta=0.5$ corresponding with $\theta=60°$ as appropriate for equilateral triangles. On the other hand, from the K-K-K correlation function follows that neighboring K^+ ions are not at the same distance from each other. This is also suggested by the broadness of the first peak of the K-K pair-correlation function. As to the K-Pb-K correlations we can distinguish two cases: either both K^+ ions are at the same side of a $(Pb_4)^{4-}$ tetrahedron or they are on different sides. The former case gives rise to a smaller K-Pb-K angle than the latter case. The K-Pb-K correlation function shows an increase towards $\cos\theta=-1$, implying that there are K-Pb-K triplets making an angle of 180°. This is also the case in the crystal structure of KPb where some of the K-Pb-K triplets consist of K atoms, of which one is at the center of a face of a particular tetrahedron while the other is at the opposite corner of that tetrahedron. The Pb-K-Pb correlation function shows a relatively narrow peak at about $\cos\theta=0.7$, well separated from a very broad maximum extending from $\cos\theta=0.5$ to nearly $\cos\theta=-1$, which is related to the second, also broad peak of the Pb-Pb pair-correlation function. The two peaks of the Pb-Pb-K correlation function that occur approximately at $\cos\theta=+0.5$ and $\cos\theta=-0.5$ and that are of the same height can be interpreted in the following way. If we isolate a Pb_4 tetrahedron from the crystal together with its four nearest K atoms, which are opposite the centers of the faces of the Pb_4 tetrahedron and which constitute a nearly regular tetrahedron themselves, we find that we can make Pb-Pb-K triplets having angles of approximately 60° and 120° and that there are as many combinations of 60° as 120°. Both peaks of the Pb-K-K correlation function are slightly shifted to smaller angles with respect to those denoted by the vertical bars. Again this is probably due to the broad distribution of nearest-neighbor K-K distances. The Pb-CM-Pb correlation function shows a peak at $\cos\theta=-0.33$, which is consistent with the definition of CM being the center of mass of a Pb_4 tetrahedron. The two peaks of the K-CM-K correlation function correspond with pairs of K^+ ions lying at the same or at different sides of a tetrahedron and are well predicted by the calculations based on the peak positions of the CM-K and K-K pair-correlation functions. Just like the correlation function of K-Pb-K triplets, the Pb-CM-K correlation function indicates that the Pb^- ions, the centers of mass, and the K^+ ions of some of the Pb-CM-K triplets are collinear.

In the above analysis we have seen that K^+ ions are preferably situated at the faces of a Pb_4 tetrahedron. From the crystal structure we know that there is a second shell at a somewhat larger distance from the center of mass containing K atoms that are lying opposite the corners of the tetrahedron. To find out if this also occurs in the liquid, we have calculated the K-CM-K and Pb-CM-K correlation functions using as cutoff distance the one defined by the second minimum of the CM-K pair-correlation function. They are shown in the lowest-lying plot of Fig. 6. The ratio of the peak heights at smaller angle relative to that at larger angle has increased compared with the previously calculated K-CM-K correlation function. This implies that the number of K-CM-K combinations where both K^+ ions are nearest neighbors has increased. Moreover, the Pb-CM-K correlation function shows a distinct increase towards $\cos\theta=0$. This is a clear indication for the presence of K^+ at the corners of a $(Pb_4)^{4-}$ polyanion.

F. Bhatia-Thornton partial structure factors

If we assume the $(Pb_4)^{4-}$ polyanions to be single particles and leave their internal structure out of consideration, it makes sense to apply the Bhatia-Thornton (BT) formalism,[27] which is the appropriate way to investigate the structural aspects of (ionic) order-disorder phenomena in binary liquids. For this purpose we have used the pair-correlation functions involving the centers of mass of the $(Pb_4)^{4-}$ ions instead of those related to the individual Pb^- ions. Figure 7 shows the BT partial structure factors of KPb and CsPb. They have been found by Fourier transformation according to

$$S_{NN}(q)=1+4\pi\rho_0'\int_0^\infty r^2[g_{NN}(r)-1]\frac{\sin(qr)}{qr}dr\ , \quad (11a)$$

$$S_{NC}(q)=4\pi\rho_0'\int_0^\infty r^2 g_{NC}(r)\frac{\sin(qr)}{qr}dr\ , \quad (11b)$$

and

$$S_{CC}(q)=\rho_A\rho_{CM}/\rho_0'^2+4\pi\rho_0'\int_0^\infty r^2 g_{CC}(r)\frac{\sin(qr)}{qr}dr\ , \quad (11c)$$

where ρ_A and ρ_{CM} are the number densities of the A^+ and $(Pb_4)^{4-}$ ions, respectively, and $\rho_0'=\rho_A+\rho_{CM}$. The

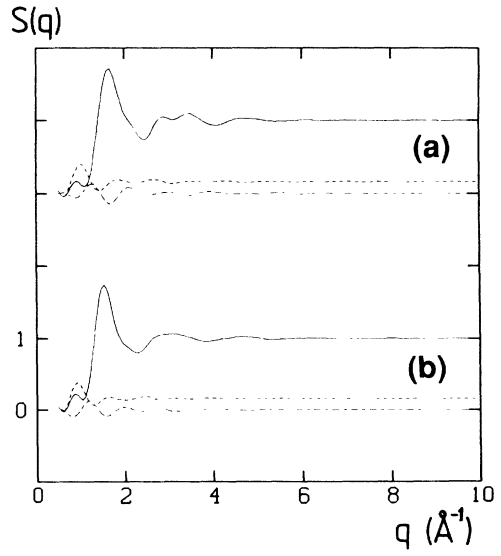

FIG. 7. The Bhatia-Thornton partial structure factors $S_{NN}(q)$ (solid), $S_{CC}(q)$ dashes, and $S_{NC}(q)$ (long-short dashes) of KPb at (a) 870 K and CsPb at (b) 930 K.

functions $g_{NN}(r)$, $g_{NC}(r)$, and $g_{CC}(r)$ describe the correlations of density (N) and concentration (C) fluctuations and are calculated from $g_{\mathrm{CMCM}}(r)$, $g_{\mathrm{CM}A}(r)$, and $g_{AA}(r)$ as follows:[28]

$$g_{NN}(r)=[(\rho_A/\rho_0')^2 g_{AA}(r)+(\rho_{\mathrm{CM}}/\rho_0')^2 g_{\mathrm{CMCM}}(r) +2(\rho_A\rho_{\mathrm{CM}}/\rho_0'^2)g_{\mathrm{CM}A}(r)] , \quad (12a)$$

$$g_{NC}(r)=(\rho_A\rho_{\mathrm{CM}}/\rho_0'^2)\{(\rho_A/\rho_0')g_{AA}(r) -(\rho_{\mathrm{CM}}/\rho_0')g_{\mathrm{CMCM}}(r) +[(\rho_{\mathrm{CM}}-\rho_A)/\rho_0']g_{\mathrm{CM}A}(r)\} , \quad (12b)$$

and

$$g_{CC}(r)=(\rho_A\rho_{\mathrm{CM}}/\rho_0'^2)^2[g_{AA}(r)+g_{\mathrm{CMCM}}(r)-2g_{\mathrm{CM}A}(r)] . \quad (12c)$$

They are plotted in Fig. 8. Clearly, the structure is dominated by the density fluctuations. A maximum in $g_{CC}(r)$ implies that like atoms are preferred as nearest neighbors, while a minimum in $g_{CC}(r)$ corresponds to a preference for unlike atoms. Since the first peak of $g_{NN}(r)$ coincides with a minimum of $g_{CC}(r)$, it is due to correlations between A^+ and $(Pb_4)^{4-}$ ions. Oppositely, the second peak of $g_{NN}(r)$ corresponds with correlations between $(Pb_4)^{4-}$ ions among each other as well as A^+ ions among each other. It can be shown that the maximum of $g_{CC}(r)$ at this position yields the prepeak at about 1 $Å^{-1}$ in $S_{CC}(q)$, using the same kind of arguments as at the end of Sec. III C.

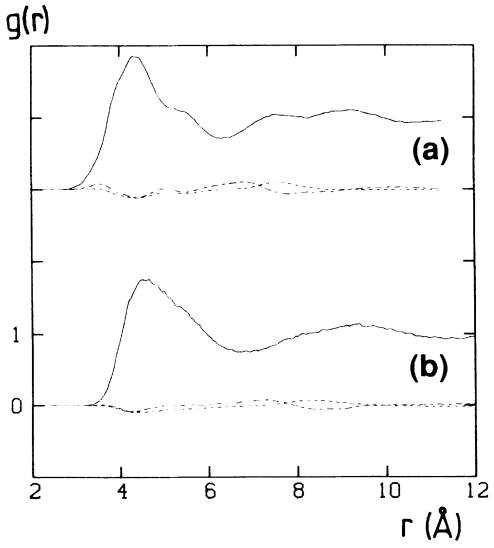

FIG. 8. The correlation functions $g_{NN}(r)$ (solid), $g_{CC}(r)$ (dashes), and $g_{NC}(r)$ (long-short dashes) of KPb at (a) 870 K and CsPb at (b) 930 K.

TABLE V. Diffusion constants (in units of 10^{-5} cm^2/s).

	D_A	D_{Pb}	D_{CM}
NaPb	0.33	0.17	0.067
KPb	1.3	0.53	0.18
RbPb	1.2	0.58	0.19
CsPb	4.4	1.3	0.49

G. Final remarks

Finally, we have calculated the self-diffusion constants D of the A^+, Pb^-, and $(Pb_4)^{4-}$ ions (Table V). As is to be expected, the values of D decrease in the above-mentioned order for a given system. The diffusion constants of KPb do not differ much from those of RbPb, but are about three times as large as those of NaPb, while there is a jump in their values when going from RbPb to CsPb.

We would like to make several suggestions for modifications of the potential that might be the subject of a future MD study. The temperature-dependent properties such as the specific-heat capacity[29] may be studied by using an anharmonic Morse potential[30] instead of the harmonic potential of Eq. (3) to allow for dissociation of the Pb_4 tetrahedra. The alkali and Pb atoms have a relatively large electronic polarizability (see, e.g., Ref. 2). Consequently, the interactions due to polarization should not be neglected and should be taken into account either by including the van der Waals terms in the original BMH potential,[19] or by treating the induced dipole moments as dynamical variables.[10] A study of the dynamics of these systems has already been reported.[31]

IV. CONCLUSIONS

In this paper we have presented the results of a series of MD calculations for liquid NaPb, KPb, RbPb, and CsPb. The main conclusions are as follows.

(1) A simple ionic-molecular model can account for the structure factors measured by neutron diffraction better than the previously reported model calculations.[1]

(2) Only a fraction of the Pb atoms in NaPb is clustered as Pb_4 tetrahedra. This is consistent with the experimental observation mentioned before that the behavior of NaPb resembles both that of ionic Li-Pb and that of Pb_4-forming K-Pb. It is also consistent with measurements of the heat capacity: those of KPb, RbPb, and CsPb show anomalous temperature dependence upon melting, which can be explained by assuming a dissociation of Pb_4 units, while the heat capacity of liquid NaPb hardly deviates from typical metallic values.[29]

(3) The peak positions of the pair-correlation functions agree well with the corresponding distances from the known crystal structures. Similarly, the calculated coordination numbers are very close to those of the solid.

(4) From an analysis of the triplet correlation functions, it follows that the spatial distribution of alkali

atoms around a Pb_4 tetrahedron in both liquid and solid is much alike. More specifically, we have found that an anisotropy occurs due to steric effects: the alkali atoms centered at the faces are closer to the center of mass of the Pb_4 tetrahedron compared with those at the corners.

ACKNOWLEDGMENTS

This work forms part of the research program of the Stichting voor Fundamenteel Onderzoek der Materie (Foundation for Fundamental Research on Matter, FOM) and was made possible by financial support from the Nederlandse Organisatie voor Zuiver Wetenschappelijk Onderzoek (The Netherlands Organization for the Advancement of Pure Research, ZWO). One of us (M.-L.S.) gratefully acknowledges the support of the U.S. Department of Energy Division of Materials Sciences of the Office of Basic Energy Sciences, under Contract No. W-31-109-ENG-38. Another (H.T.J.R.) gratefully acknowledges the support of Argonne National Laboratory, which allowed access to their computer facilities from The Netherlands. Computing time was made available by the U.S. Department of Energy (Office of Basic Energy Sciences), on the ER-Cray supercomputer at Lawrence Livermore Laboratory.

[1]H. T. J. Reijers, M.-L. Saboungi, D. L. Price, J. W. Richardson, Jr., and K. J. Volin, Phys. Rev. B **40**, 6018 (1989).

[2]W. Geertsma, J. Dijkstra, and W. van der Lugt, J. Phys. F **14**, 1833 (1984).

[3]W. van der Lugt and W. Geertsma, J. Non-Cryst. Solids **61-62**, 187 (1984); W. van der Lugt and W. Geertsma, Can. J. Phys. **65**, 326 (1987).

[4]J. A. Meijer, W. Geertsma, and W. van der Lugt, J. Phys. F **15**, 899 (1985); J. A. Meijer, G. J. B. Vinke, and W. van der Lugt, *ibid.* **16**, 845 (1986).

[5]S. Matsunaga, T. Ishiguro, and S. Tamaki, J. Phys. F **13**, 587 (1983); M.-L. Saboungi, S. J. Herron, and R. Kumar, Ber. Bunsenges. Phys. Chem. **89**, 375 (1985); M.-L. Saboungi, S. R. Leonard, and J. Ellefson, J. Chem. Phys. **85**, 6072 (1986); P. J. Tumidajski, A. Petric, T. Takenaka, M.-L. Saboungi, and A. D. Pelton, J. Phys. Condens. Matter **2**, 209 (1990).

[6]R. E. Marsh and D. P. Shoemaker, Acta Crystallogr. **6**, 197 (1953).

[7]I. F. Hewaidy, E. Busmann, and W. Klemm, Z. Anorg. (Allg.) Chem. **328**, 283 (1964).

[8]F. Springelkamp, R. A. de Groot, W. Geertsma, W. van der Lugt, and F. M. Mueller, Phys. Rev. B **32**, 2319 (1985).

[9]W. Geertsma and J. Dijkstra, J. Phys. C **18**, 5987 (1985).

[10]M.-L. Saboungi, A. Rahman, J. W. Halley, and M. Blander, J. Chem. Phys. **88**, 5818 (1988).

[11]M. J. L. Sangster and M. Dixon, Adv. Phys. **25**, 247 (1976).

[12]A. Rahman, Phys. Rev. Lett. **32**, 52 (1974); A. Rahman, Phys. Rev. A **9**, 1667 (1974).

[13]T. Lee, J. Bisschop, W. van der Lugt, and W. F. van Gunsteren, Physica B+C (Amsterdam) **93B**, 59 (1978).

[14]M. J. Huijben, W. van der Lugt, W. A. M. Reimert, J. Th. M. de Hosson, and C. van Dijk, Physica B+C (Amsterdam) **97B**, 338 (1979).

[15]G. Jacucci, M. Ronchetti, and W. Schirmacher, *Condensed Matter Research Using Neutrons,* edited by S. W. Lovesey and R. Scherm (Plenum, New York, 1984).

[16]A. P. Copestake, R. Evans, H. Ruppersberg, and W. Schirmacher, J. Phys. F **13**, 1993 (1983).

[17]J. Hafner, J. Phys. Condens. Matter **1**, 1133 (1989).

[18]R. Car and M. Parrinello, Phys. Rev. Lett. **55**, 2471 (1985); in *Proceedings of the 18th International Conference on the Physics of Semiconductors, 1986,* edited by O. Engström (World Scientific, Singapore, 1987), p. 1165; Phys. Rev. Lett. **60**, 204 (1988).

[19]M. L. Huggins and J. E. Mayer, J. Chem. Phys. **1**, 643 (1933).

[20]M. P. Tosi and F. G. Fumi, J. Phys. Chem. Solids **25**, 31 (1964); **25**, 45 (1964).

[21]L. Verlet, Phys. Rev. **159**, 98 (1967).

[22]P. P. Ewald, Ann. Phys. (Leipzig) [Folge 4] **21**, 1087 (1921).

[23]N. F. Sears, *Methods of Experimental Physics,* edited by D. L. Price and K. Sköld (Academic, London, 1986), Vol. 23A.

[24]L. Pauling, *The Nature of the Chemical Bond* (Cornell University Press, New York, 1960).

[25]H. Bürger and R. Eujen, Z. Anorg. Allg. Chemie **394**, 19 (1972).

[26]P. Vashishta, R. K. Kalia, and I. Ebbsjö, Phys. Rev. B **39**, 6034 (1989).

[27]A. B. Bhatia and D. E. Thornton, Phys. Rev. B **2**, 3004 (1970).

[28]N. H. March and M. P. Tosi, *Atomic Dynamics in Liquids* (MacMillan, London, 1976).

[29]M.-L. Saboungi, H. T. J. Reijers, M. Blander, and G. K. Johnson, J. Chem. Phys. **89**, 5869 (1988).

[30]K. Toukan and A. Rahman, Phys. Rev. B **31**, 2643 (1985).

[31]K. Toukan, H. T. J. Reijers, C.-K. Loong, D. L. Price, and M.-L. Saboungi, Phys. Rev. B **41**, 11 739 (1990).